Bioscience of Microbiota, Food and Health Vol. 43 (4), 367–380, 2024

Full Paper

Lactobacillus acidophilus CICC 6075 attenuates high-fat diet-induced obesity by improving gut microbiota composition and histidine biosynthesis

Shenyang ZHANG[1, 2a], Shuai YANG[3a], Yun ZHUANG[3a], Dan YANG[3], Xiqun GU[3], Yi WANG[3], Zhenzhen WANG[4], Renjin CHEN[3*] and Fuling YAN[1*]

[1]*School of Medicine, Southeast University, Nanjing, Jiangsu 210009, China*
[2]*Department of Neurology, Affiliated Hospital of Xuzhou Medical University, Xuzhou, Jiangsu, China*
[3]*College of Life Sciences, Xuzhou Medical University, Xuzhou, Jiangsu, China*
[4]*Cancer Institute, Xuzhou Medical University, Xuzhou, Jiangsu, China*

Received February 1, 2024; Accepted June 4, 2024; Published online in J-STAGE June 21, 2024

This study aimed to investigate the potential anti-obesity efficacy of *Lactobacillus acidophilus* CICC 6075. The study analyzed fecal metagenomic data from 120 obese and 100 non-obese individuals. C57BL/6 mice on normal diet or high-fat diet (HFD) were treated with *L. acidophilus* CICC 6075 by daily oral gavage for 12 weeks, followed by evaluations of the obesity phenotype. Metagenomic analysis revealed depletion of *L. acidophilus* in obese individuals. Administration of *L. acidophilus* CICC 6075 attenuated excessive weight gain and fat accumulation and maintained the intestinal barrier in HFD-induced obese mice. Sequencing results showed that HFD hindered α- and β-diversity while reducing the relative abundance of *Lactobacillus* and *norank_f_Muribaculaceae* and significantly increasing the relative abundance of *Ileibacterium*. *L. acidophilus* CICC 6075 reversed these results and reduced the Firmicutes/Bacteroidetes ratio. Supplementation of *L. acidophilus* CICC 6075 enhanced histidine biosynthesis, inhibited the NF-κB pathway, and significantly reduced the expression levels of inflammatory factors in adipose tissue. These results indicate that *L. acidophilus* CICC 6075 alleviates HFD-induced obesity in mice by inhibiting the activation of the NF-κB pathway and enhancing gut microbiota functionality. This suggests that *L. acidophilus* CICC 6075 may be a good candidate probiotic for preventing obesity.

Key words: *Lactobacillus acidophilus*, obesity, histidine, gut microbiota

INTRODUCTION

Obesity is a significant health issue that has garnered much attention, and recent data indicate that nearly 30% of the global population consists of overweight or obese individuals [1, 2]. During clinical observations, obesity often presents with changes in body shape and is strongly correlated with lipid metabolic dysfunction, chronic inflammation, and oxidative stress. Furthermore, obesity is a recognized risk factor for various diseases, including cancer, glucose intolerance, and coronary artery disease [3–5]. Drugs used clinically to combat obesity have restricted efficacy and notable adverse reactions [6–10]. Efficient and secure therapeutic approaches for obesity have not yet been determined.

The gut microbiota impacts the process of obtaining nutrients, regulating energy, and storing fat [11, 12]. Recent studies have suggested that an imbalance in natural gut bacteria, referred to as dysbiosis, could contribute to an increased risk of obesity [13–15]. Probiotics release advantageous substances such as short-chain fatty acids, amino acids, and vitamins. They also produce compounds that have anti-inflammatory and antioxidant properties, which help to control the body's energy metabolic processes and maintain a balanced metabolism and energy level [16–18].

Lactobacillus acidophilus is widely and frequently used as a probiotic. Oral administration of *L. acidophilus* controls the process of breaking down fats, enhances the body's ability to respond to insulin, prevents inflammation and oxidative stress, and maintains a balanced state of the microorganisms in the

[a]These authors contributed equally to this work and share first authorship.
*Corresponding authors. Fuling Yan (E-mail: yanfuling12@163.com); Renjin Chen (E-mail: crj@xzhmu.edu.cn)
(Supplementary materials: refer to PMC https://www.ncbi.nlm.nih.gov/pmc/journals/2480/)

doi: 10.12938/bmfh.2024-008

intestines, resulting in many health advantages [19–24]. *L. acidophilus* CICC 6075 modulates the activity of β-galactosidase, and accumulation of senescent adipocytes is crucial in initiating pathological remodeling and disrupting the energy balance in adipose tissue [25, 26]. However, the related mechanisms of *L. acidophilus* CICC 6075 against obesity have not yet been reported.

Histidine levels have been linked to obesity, heart failure, and chronic renal disease [27, 28]. Among the many characteristics of histidine are its anti-inflammatory and antioxidant qualities. Supplementation with histidine and histidine-containing dipeptides may provide protection against high-fat diet (HFD)-induced obesity in mice by ameliorating obesity and regulating blood glucose [29]. Supplementation with histidine reduces ethanol-induced liver damage; however, it is unclear how this affects metabolic processes [29, 30]. Histidine supplementation has been shown in clinical trials to enhance insulin by downregulating inflammatory resistance in women with non-alcoholic fatty liver disease [31]. However, little is understood about the function of histidine in obesity and its possible processes. It is important to note that the gut microbiota has been implicated in chronic inflammatory processes leading to obesity and regulates the bioavailability of dietary histidine [32]. It is unclear whether there is a link between the gut microbiota, histidine metabolism, and obesity.

Thus, this study aimed to evaluate the effects of *L. acidophilus* CICC 6075 on lipid metabolism, the intestinal barrier, and intestinal flora in HFD-induced obese mice. In this present study, *L. acidophilus* CICC 6075 alleviated HFD-induced obesity in mice by inhibiting the activation of the NF-κB pathway and enhancing gut microbiota functionality.

MATERIALS AND METHODS

Study inclusion and data acquisition

We searched PubMed for studies that published fecal shotgun metagenomic data from normal-weight controls (n=100) and patients with obesity (n=120). The raw data were categorized based on the obesity classification of the World Health Organization (WHO). In brief, individuals were designated as part of the normal group if their body mass index (BMI) was less than 25 kg/m^2. Conversely, individuals were classified as part of the obesity group if their BMI was 30 kg/m^2 or higher and they concurrently presented with at least one comorbidity, such as type 2 diabetes mellitus, hypertension, or obstructive cardiovascular disease. Raw FASTQ files from two investigations were obtained by downloading them from the Sequence Read Archive (SRA) database of the National Center for Biotechnology Information (NCBI) using the following NCBI identifiers: PRJEB12123 for Liu *et al.* [33] and PRJEB14215 for Hoyles *et al.* [34].

Study design

Male C57BL/6 J mice (8 weeks old; weight, 25–28 g; n=12) were purchased from GemPharmatech LLC (Nanjing, Jiangsu, China). The mice were housed at a facility at Xuzhou Medical University (Xuzhou, Jiangsu, China) and maintained under a 12-hr light–dark cycle at constant temperature and humidity (23 ± 1°C and 55–65%, respectively) with free access to water and the same quality of food. Mice were fed either a normal chow diet (NCD; 10% kcal fat; Jiangsu Xietong Pharmaceutical Bio-engineering Co., Ltd., Nanjing, China) or an HFD (60% kcal fat, Jiangsu Xietong Pharmaceutical Bio-engineering Co., Ltd.) *ad libitum* for 12 weeks (Fig. 1). In order to reduce potential bias, this study used a randomization method to randomly divide mice into four groups (n=3): NCD-fed control group (NCD), HFD-fed phosphate-buffer saline (PBS)-treated group (HFD), HFD-fed with *L. acidophilus*-treated group (HFD-L), and HFD-fed with heat-killed *L. acidophilus*-treated group (HFD-H). At the end of the experimental period, mice were subjected to a 12-hour fasting period and then anesthetized using an isoflurane chamber (RWD, Shenzhen, China) before collecting organs and blood samples.

Culture and administration of L. acidophilus *CICC 6075*

L. acidophilus CICC 6075 was acquired from the China Industrial Microbial Strain Collection and Management Center (CICC; Beijing, China). The strain was isolated from the gastrointestinal tract and cultured in De Man, Rogosa, and Sharpe (MRS) medium for a duration of 48 hr at 37°C while maintaining anaerobic conditions. The bacterial concentration was determined by quantifying the absorbance at a wavelength of 600 nm. The C57BL/6 J mice (NCD and HFD) were gavaged 200 μL of PBS every day. C57BL/6 J mice fed the HFD were orally gavaged with 1×10^9 CFU or 1×10^9 CFU of heat-killed *L. acidophilus* CICC 6075 in 200 μL of PBS at the same time every day. *L. acidophilus* CICC 6075 was subjected to heat treatment at 121°C under 225-kPa pressure for 15 min, resulting in its inactivation.

Tissue extraction and hematoxylin and eosin staining

After completion of the experiment, the mice were euthanized. Liver, fat, and intestinal tissues were carefully extracted and weighed while their physical appearance was observed. Liver and colon tissues were subsequently fixed in paraffin for 24 hr before being sliced into 3-μm sections and stained with hematoxylin for 10 min to highlight nuclei, and then the sections were washed in tap water. Next, the slides were transferred to a staining jar containing eosin solution for 3 sec and washed again with tap water. The slides were then dehydrated using a sequential procedure including 80% ethanol for 20 sec, 90% ethanol for 20 sec, 95% ethanol for 20 sec, 100% ethanol for 5 min, and xylene for 5 min. After being extracted from the xylene, the slides were allowed to desiccate in a fume hood. Images of hematoxylin and eosin (HE) staining were obtained using an inverted microscope that was coupled with a digital microscope (Olympus, Tokyo, Japan).

Histopathology analysis

The severity of nonalcoholic fatty liver disease (NAFLD) activity scores was assessed using the steatosis, activity, and fibrosis (SAF) scoring system [35]. Steatosis, inflammatory infiltrates, and ballooning were quantified, and NAFLD grades were determined. Steatosis was categorized into grades 0–3 based on the percentage of intracytoplasmic lipid droplets in the liver parenchyma (grade 0, <5%; grade 1, 5–33%; grade 2, 34–66%; grade 3, >67%). Inflammatory infiltrates were categorized into grades 0–3 based on the number of inflammatory cell foci per 200× field of view (grade 0, 0 foci; grade 1, 1–2 foci; grade 2, 3–4 foci; grade 3, >4 foci). Ballooning lesions were categorized into grades 0–3 based on the morphology and number of ballooning hepatocytes per 200× field of view (grade 0, normal hepatocytes; grade 1, presence of round and pale cytoplasmic hepatocytes;

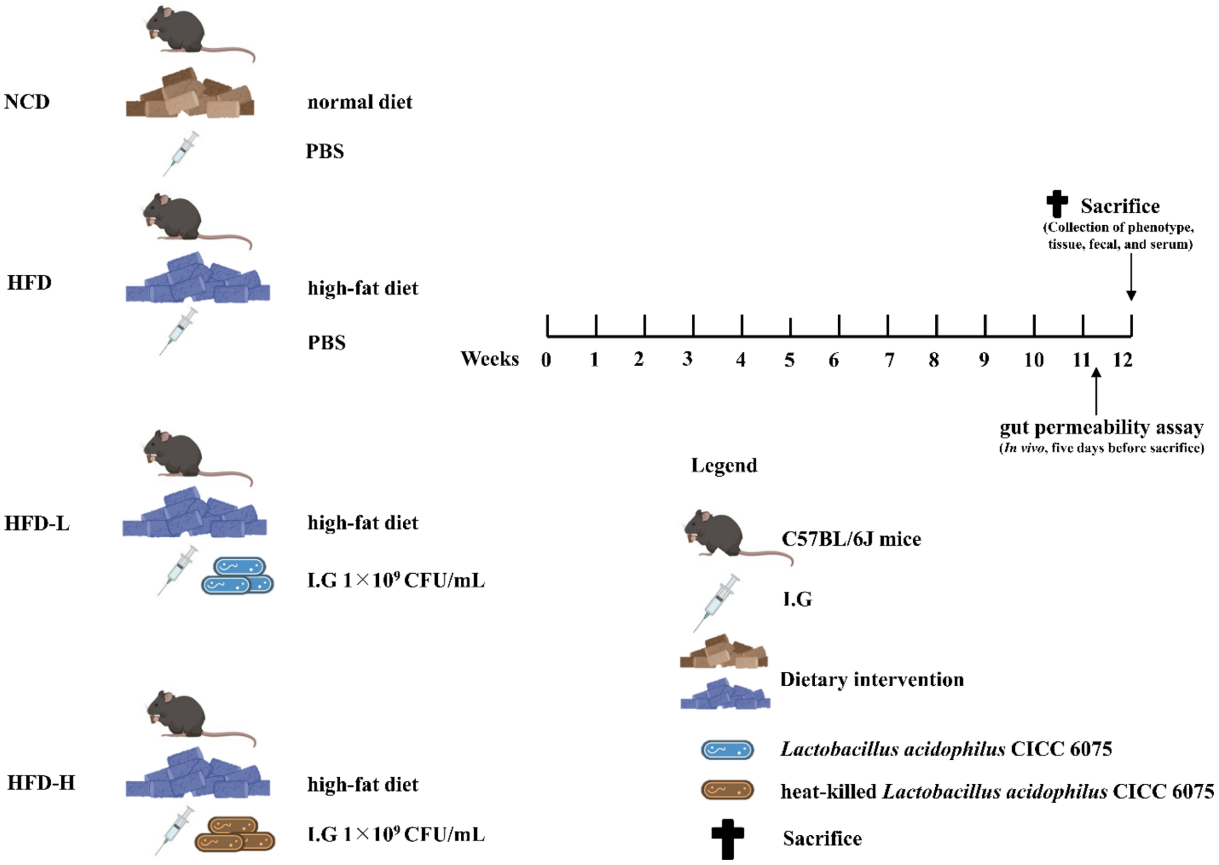

Fig. 1. Experimental design timeline.

NCD: normal chow diet; HFD: high-fat diet; HFD-L: HFD-fed with *L. acidophilus*-treated group; HFD-H: HFD-fed with heat-killed *L. acidophilus*-treated group; PBS: phosphate-buffer saline.

grade 2, one enlarged ballooning hepatocyte; grade 3, multiple enlarged ballooning hepatocytes).

In vivo gut permeability assays

Mice were fasted for 12 hr five days prior to sacrifice and then orally administered fluorescein isothiocyanate (FITC)-labeled dextran (DX-4000 FITC, 600 mg/kg body weight; Sigma-Aldrich, St. Louis, MO, USA). Serum samples were collected by orbital blood sampling after four hours, incubated at 25°C for 30 min, and then centrifuged at 1,500 g for 20 min. The serum was diluted with PBS at a dilution ratio of 1:9. The concentration of DX-4000 FITC in the serum was measured using a fluorescence spectrophotometer (Synergy H1, BioTek, Winooski, VT, USA) at an excitation wavelength of 485 nm and an emission wavelength of 535 nm.

Measurement of histidine concentration

Serum from each group was collected when mice were sacrificed and was stored at −80°C until analysis. Acetonitrile was added to the serum sample, mixed vigorously for 1 min, and centrifuged for 5 min at 16,000 g and 4°C, and the resulting liquid above the sediment was collected. The process of modifying and separating serum amino acids was carried out by using standard chemicals (Waters, Milford, MA, USA) in accordance with the guidelines provided by the manufacturer. The separations were conducted using an ultra-performance liquid chromatography technique, specifically using a reversed-phase liquid chromatography column on a Waters UPLC I-Class machine. We used a Waters TQ-XS mass spectrometer with an electrospray ionization (ESI) probe. The temperature of the positive ESI source was adjusted to 150°C, the capillary voltage was set to 1.5 kV, and the cone voltage was maintained at 20 V. The liquid chromatography-mass spectrometry system was operated using the MassLynx software (Waters), and the software was also used for data collection and processing.

Enzyme-linked immunosorbent assay

Serum from each group was collected at the time of sacrifice and stored at −80°C until analysis. Serum levels of tumor necrosis factor-α (TNF-α), interleukin-8 (IL-8), and interleukin-6 (IL-6) were quantified by Enzyme-linked immunosorbent assay (ELISA) following the manufacturer's instructions (Nanjing Yifeixue Biotech Co., Ltd., Nanjing, China).

Real-time quantitative PCR

RNA was extracted from adipose tissue samples using an RNA-Quick Purification Kit (eSun Bio, Shanghai, China) following the manufacturer's protocol. The extracted RNA was reverse transcribed into cDNA using a RevertAid First Strand cDNA Synthesis Kit (Thermo Scientific™, Thermo Fisher Scientific, Waltham, MA, USA). Real-time polymerase chain reaction (PCR) (RT-PCR) analyses were conducted using an ABI 7900HT

doi: 10.12938/bmfh.2024-008

real-time PCR system (Applied Biosystems, San Francisco, CA, USA) with Super SYBR Green real-time quantitative PCR (qPCR) Master Mix (eSun Bio, Shanghai, China). β-actin expression was used as the reference for normalization, and results were calculated based on the comparative cycle threshold method ($2^{-\Delta\Delta CT}$). The p65 NFκB primer sequences used in this study were as follows: 5′-TGCGATTCCGCTATAAATGCG-3′ and 5′-ACAAGTTCATGTGGATGAGGC-3′. The β-actin primer sequences were as follows: 5′-CAGCCTTCCTTCTTGGGTATG-3′ and 5′-GGCATAGAGGTCTTTACGGATG-3′.

Extraction of DNA and sequencing of the 16S rRNA gene

At the last point of the experiment, fecal samples were collected. Every fecal sample was rapidly frozen in liquid nitrogen shortly after being donated and thereafter stored at a temperature of −80°C. A QIAamp Fast DNA Stool Mini Kit (Qiagen, Hilden, Germany) was used to extract bacterial genomic DNA. The PCR technique was used to amplify the V3–V4 region of the 16S rRNA gene, which was then sequenced using a MiSeq platform manufactured by Illumina (Illumina, San Diego, CA, USA). The primer sequences were as follows: 338F (5′-ACTCCTACGGGAGGCAGCA G-3′) and 806R (5′-GGACTACHVGGGTWTCTAAT-3′).

Metagenomics analysis

Adaptor contamination and low-quality reads were discarded from the raw sequencing reads, and the remaining reads were filtered to eliminate the human host DNA based on the human genome reference (hg37). We acquired 1,430 Gb of high-quality paired-end reads for 220 samples, with an average of 6.5 Gb per sample, after removing human DNA reads. The Kraken2 software was used to classify the reads from the metagenome samples. All classifications were performed using the default settings in Kraken2. The Bracken software was designed to re-estimate abundances at a fixed rank by distributing reads from higher ranks into lower ranks, based on conditional probabilities estimated from the database content. A Bracken database (100-mers) was created for the HumGut_97.5 database and used to re-estimate all abundances at the species rank.

Bioinformatic analysis

The 16S rRNA sequencing data were analyzed using Quantitative Insights into Microbial Ecology (QIIME 2 V.2021.11) [36]. The DADA2 software, which was incorporated into QIIME 2, was utilized to filter the sequencing reads and produce a feature table. Amplicon sequence variants (ASVs) were clustered at 97% identity using the search plugin, and taxonomic classification was performed using the Silva (SSU138) 16S rRNA database (V.13.8). To ensure data reliability, ASVs comprising <0.005% of the total number of sequences were excluded. The resulting data yielded an average of 32,708 reads per sample (minimum, 47,213; maximum, 56,203). The sequences were aligned using the MAFFT algorithm, and subsequently, a phylogenetic tree was created employing the FastTree plugin. The gut microbiome's diversity was assessed using q2-diversity, with a rarefied sample depth of 47,213. Finally, we employed Phylogenetic Investigation of Communities by Reconstruction of Unobserved States (PICRUSt) to estimate the metagenomes of the gut microbiome based on 16S rRNA sequences, as previously described [37].

The Kruskal–Wallis test was used to examine alpha-diversity indices, followed by pairwise Mann–Whitney U comparisons. To analyze the structural variation in microbial communities across samples, a beta-diversity analysis was conducted using the unweighted uniFrac distance and visualized via principal coordinate analysis (PCoA). The Bonferroni method was used to correct the resulting p-values. In addition, variations in unweighted uniFrac distance across groups were assessed using analysis of similarities. In order to assess the differences in the abundances of taxa at the phylum, family, and genus levels between the HFD group and the HFD-L group, we conducted one-way analysis of variance (ANOVA) and post-hoc least significant testing using GraphPad Prism 6. Furthermore, the linear discriminant analysis (LDA) effect size (LEfSe) was used to detect biomarkers for both abundant taxa and functional pathways. This was achieved by computing the LDA score (≥3.5) across different groups. A heatmap was generated using R package version 4.2.1. The PICRUSt method, which utilizes ASVs, was used to forecast the prevalence of functional categories by using Kyoto Encyclopedia of Genes and Genomes (KEGG) orthologs (KOs). The data are presented as mean values plus or minus the standard error of the mean (SEM), and statistical significance was defined as $p<0.05$.

Statistical analysis

With the exception of data collected from 16S rRNA gene sequencing, all other data were examined using GraphPad Prism 6. Mean (± SEM) values were used for the analysis. To determine statistical significance, the unpaired two-tailed Student's t-test was used for comparisons between two groups, whereas one-way ANOVA was used for comparisons between more than two groups. Statistical significance was set at $p<0.05$.

Ethics approval and consent to participate

The procedures of the animal study were performed under the ethical guidelines of the Xuzhou Medical University Laboratory Animal Ethics Management Committee (approval number 4120185). The contents of this study are in full compliance with government policy and ARRIVE guidelines.

RESULTS

Signatures of the intestinal microbiota in patients with obesity

To investigate the role of the gut microbiota in obesity, a cohort of 120 individuals with obesity and 100 normal individuals underwent metagenomic analysis of their gut microbiota. Our findings demonstrated a significant reduction in alpha-diversity, as indicated by the Shannon diversity index, in the obese group compared with that in the normal group (Fig. 2A and 2B). Moreover, the gut bacterial composition differed considerably between the two groups, as illustrated by the PCoA results (Fig. 2C). At the genus level, we observed a distinct enrichment of *Prevotella*, *Lactobacillus*, and *Alistipes* among healthy individuals, whereas these genera were less abundant in the obese group (Fig. 2D). The abundances of the top 20 species of *Lactobacillus* in each individual are presented as a heatmap (Fig. 2E). Notably, *L. acidophilus* exhibited a significantly lower relative abundance in the obese group than in the normal group (Fig. 2F). *Lactobacillus paracollinoides* and *Lactobacillus helveticus*, which were less abundant than *L. acidophilus*, did not differ between the obese and normal groups (Fig. 2G and 2I). However, the relative abundance

of *Lactobacillus heilongjiangensis* was significantly higher in the obese group than in the normal group (Fig. 2H).

Administration of L. acidophilus *CICC 6075 improved HFD-induced adiposity and fatty liver in mice*

Eight-week-old male mice were fed either NCD or HFD and orally supplemented with live or heat-killed *L. acidophilus* CICC 6075 for 12 weeks. HFD-L mice showed a notable decrease in

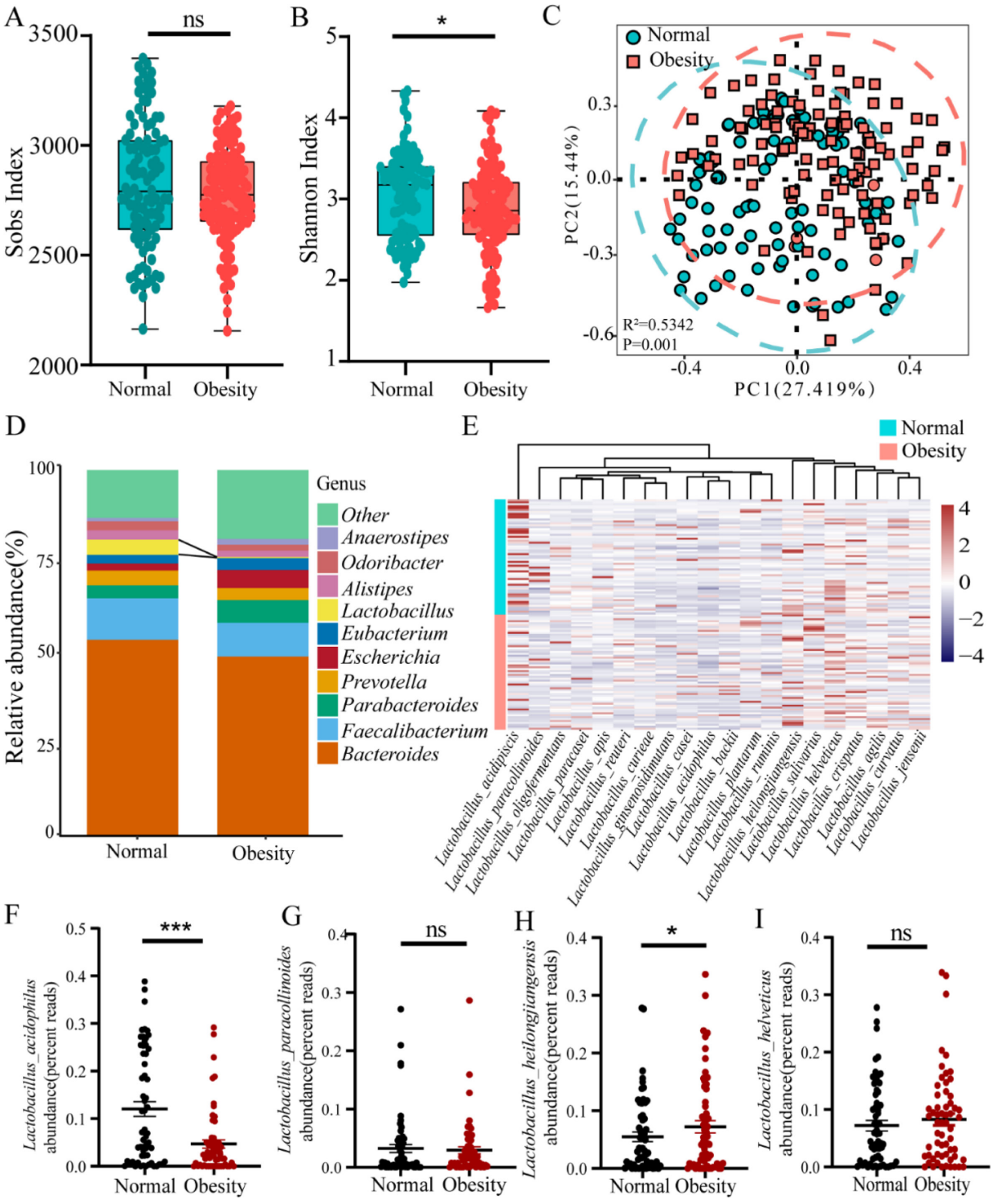

Fig. 2. Composition of the fecal microbiota of obese and normal individuals. (**A, B**) Sobs index and Shannon index of the normal and obesity groups at the species level. (**C**) PCoA of fecal microbiota from the normal and obesity group individuals using the Bray–Curtis (R^2=0.5342, p=0.001) distance. (**D**) The relative abundances of the top 10 bacteria at genus level. (**E**) Heatmap of strains of different species of *Lactobacillus* according to relative abundance. **(F–I)** Relative abundance (percent reads) of predominant bacteria of the *Lactobacillus*. Data are expressed as mean ± SEM. Normal individuals, *n*=100; obese individuals, *n*=120. *p<0.05; **p<0.01, and ***p<0.001. ns: not significant; SEM: standard error of mean.

doi: 10.12938/bmfh.2024-008

body weight gain (by ~40%; Fig. 3A and 3B), total white adipose tissue (by 45%; Fig. 3C), and total white fat weight/body weight and liver weight/body weight ratios compared with those of HFD-fed mice (Fig. 3D and 3E). We found a significant difference in food intake between the high-fat diet and normal diet control groups, but no difference was found in the three groups with high-fat diet-induced obesity, suggesting that supplementation with *L. acidophilus* did not alleviate obesity by affecting food intake in mice (Supplementary Fig. 1D). Although HFD mice and HFD-H mice exhibited similar trends to HFD-L mice, there was no statistically significant impact on the overall weight of white adipose tissue and liver (Fig. 4A–4C).

To study the impact of *L. acidophilus* CICC 6075 on the accumulation of lipids in tissues, histological analysis was conducted on tissue sections. HFD-L mice showed a significant enhancement in liver appearance and a 39% decrease in the accumulation of lipids in the liver compared with HFD-fed obese mice (Fig. 4D). Another key finding was that the mean area of adipocytes in the adipose tissue of the epididymis was significantly higher in the HFD group than in the NCD group. In addition, the mean adipocyte area was significantly lower in HFD-L mice than in HFD mice, but there was no difference in the mean adipocyte area between HFD-H and HFD mice (Fig. 4E).

Given that intestinal dysbiosis in HFD-fed animals may affect gut permeability, thereby causing the release of bacterial lipopolysaccharide (LPS) into the circulation [38], we investigated whether *L. acidophilus* CICC 6075 modulates gut integrity. Our results showed that *in vivo* intestinal permeability, as determined by oral administration of DX-4000-FITC followed by measurement of its circulating concentration, was significantly higher in the HFD group than in the NCD group and that HFD-induced increases in intestinal permeability and intestinal mucosal disruption were blocked by *L. acidophilus* CICC 6075 treatment (Fig. 4F). The HFD-L and HFD-H groups did not show significant differences compared with the NCD group. Nevertheless, the administration of *L. acidophilus* CICC 6075 entirely reversed these effects. The expression levels of the tight junction proteins Claudin-1 and ZO-1 were significantly lower in the HFD group compared with the NCD group. Furthermore, supplementation with L. acidophilus CICC 6075 significantly up-regulated their expression, which was not observed with supplementation with heat-killed L. acidophilus CICC 6075 (Fig. 4G–4I). This is consistent with the results of HE staining and *in vivo* intestinal permeability. The findings indicate that *L. acidophilus* CICC 6075 may significantly decrease weight gain and accumulation of lipids while also repairing the intestinal barrier in HFD-fed mice.

Effects of L. acidophilus *CICC 6075 on gut microbial diversity and richness*

The gut microbiota of obese individuals and HFD-fed mice exhibit decreased alpha-diversity, modified beta-diversity, higher ratios of Firmicutes to Bacteroides, increased abundances of bacteria that produce endotoxins, and decreased numbers of bacteria with stable immunological properties [39–41]. The

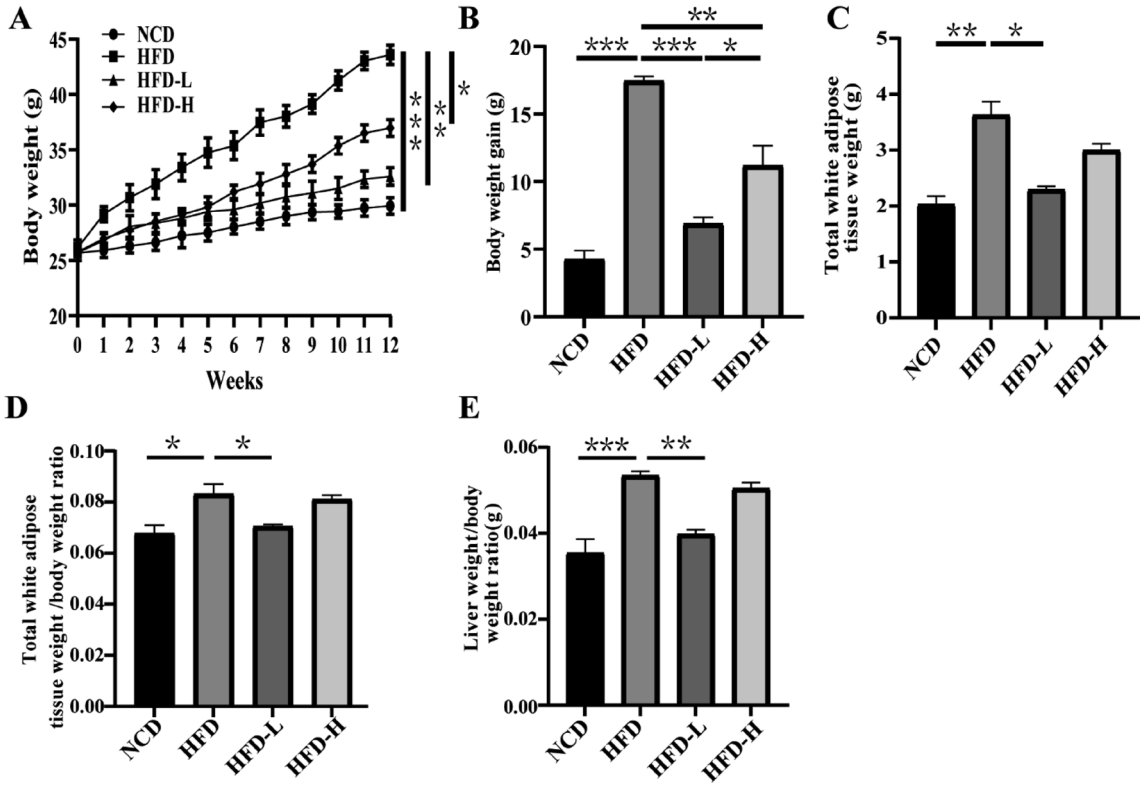

Fig. 3. *L. acidophilus* CICC 6075 ameliorated body weight and fat accumulation in HFD-fed mice. Effects of *L. acidophilus* CICC 6075 treatment on (**A**) body weight evolution, (**B**) body weight gain, (**C**) total white adipose tissue weight, (**D**) total white adipose tissue weight/body weight ratio, and (**E**) liver weight/body weight ratio. Data are expressed as mean ± SEM (n=3). *p<0.05; **p<0.01, and ***p<0.001. NCD: normal chow diet; HFD: high-fat diet; HFD-L: HFD-fed with *L. acidophilus*-treated group; HFD-H: HFD-fed with heat-killed *L. acidophilus*-treated group; SEM: standard error of mean.

doi: 10.12938/bmfh.2024-008

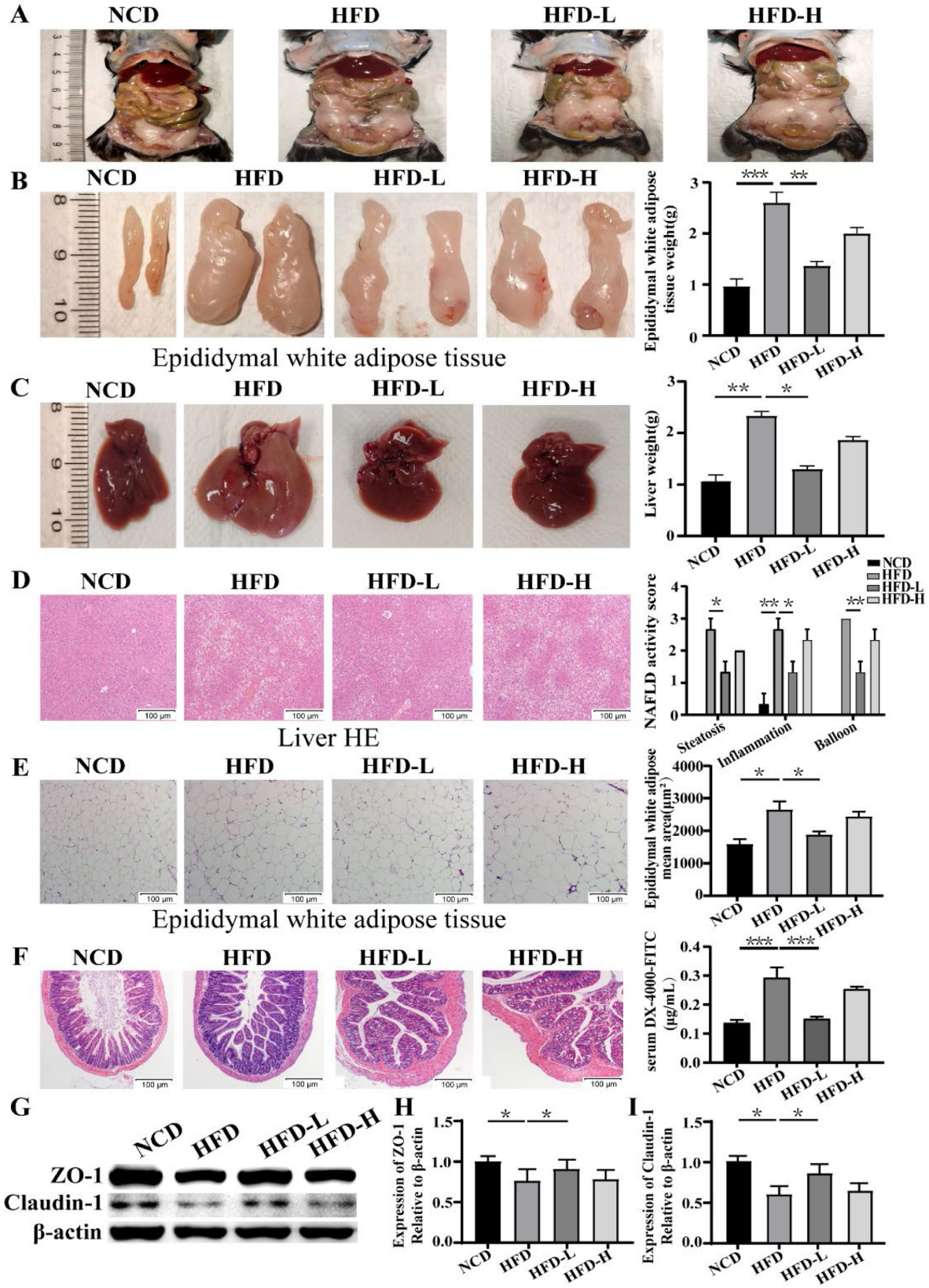

Fig. 4. *L. acidophilus* CICC 6075 restored morphological changes in HFD-fed mice. Effects of *L. acidophilus* CICC 6075 treatment: (**A**) abdominal photograph, (**B**) epididymal white adipose tissue (WAT) photograph and weight, (**C**) liver photograph and weight, (**D**) photographs of HE-stained sections of livers and steatosis grade, (**E**) epididymal white adipocyte morphology and mean area in the same field of view, and (**F**) photographs of HE-stained sections of the intestine and intestinal permeability assay. (**G–I**) ZO-1 and Claudin-1 expression was determined by Western blot and normalized to actin. Data are expressed as mean ± SEM (n=3). *p<0.05; **p<0.01, and ***p<0.001. NCD: normal chow diet; HFD: high-fat diet; HFD-L: HFD-fed with *L. acidophilus*-treated group; HFD-H: HFD-fed with heat-killed *L. acidophilus*-treated group; SEM: standard error of mean.

doi: 10.12938/bmfh.2024-008

impact of *L. acidophilus* CICC 6075 on the microbial composition was investigated by analyzing bacterial 16S rRNA gene sequences (V3–V4 region) in feces using a MiSeq sequencing-based analysis.

The bacterial libraries derived from our samples effectively captured the diversity of the microbial communities, as evidenced by the near-saturation of the rarefaction curves (Fig. 5A). To assess differences in microbial composition, we used PCoA to calculate beta-diversity (Fig. 5B). The overall composition of the gut flora differed significantly among the groups according to ANOVA. Additionally, alpha-diversity indicators, such as richness and diversity (measured using the Sobs and Shannon indices, respectively), were computed. HFD feeding had a profound impact on gut microbial alpha-diversity, resulting in a marked decrease (Fig. 5C and 5D), whereas supplementation with *L. acidophilus* CICC 6075 effectively restored these levels.

To gain a better understanding of the shared richness among each group and to assess the extent of variation in the samples, we performed hierarchical clustering and generated a Venn diagram to illustrate the overlap between groups. At the genus level, there was less variation in microbial composition within the groups (Supplementary Fig. 2A). Among the 995 ASVs, only 152 were common to all groups. Additionally, 367 ASVs were shared between any two of the four groups, while 476 ASVs were unique to each individual group. (Supplementary Fig. 2B). Furthermore, the analysis revealed that *L. acidophilus* CICC 6075 treatment significantly alleviated the decrease in the number of ASVs in HFD-fed mice, indicating that it had a positive impact on the richness and diversity of the intestinal microbiota. These results highlight the significance of *L. acidophilus* CICC 6075 treatment on the richness and diversity of the intestinal microbiota.

Effects of L. acidophilus *CICC 6075 on the gut microbiota composition*

The ratio of saprophytes to bacteria is commonly used to indicate dysbiosis of the gut flora, which is linked to obesity and related diseases [42]. Feeding on an HFD had a significant impact on the relative abundance of Firmicutes and the Firmicutes/Bacteroidetes ratio when compared with that in the NCD group (Supplementary Fig. 3A and 3B). Notably, treatment with *L. acidophilus* CICC 6075 in HFD-fed mice, particularly in the HFD-L group, reduced the relative abundance of Firmicutes and

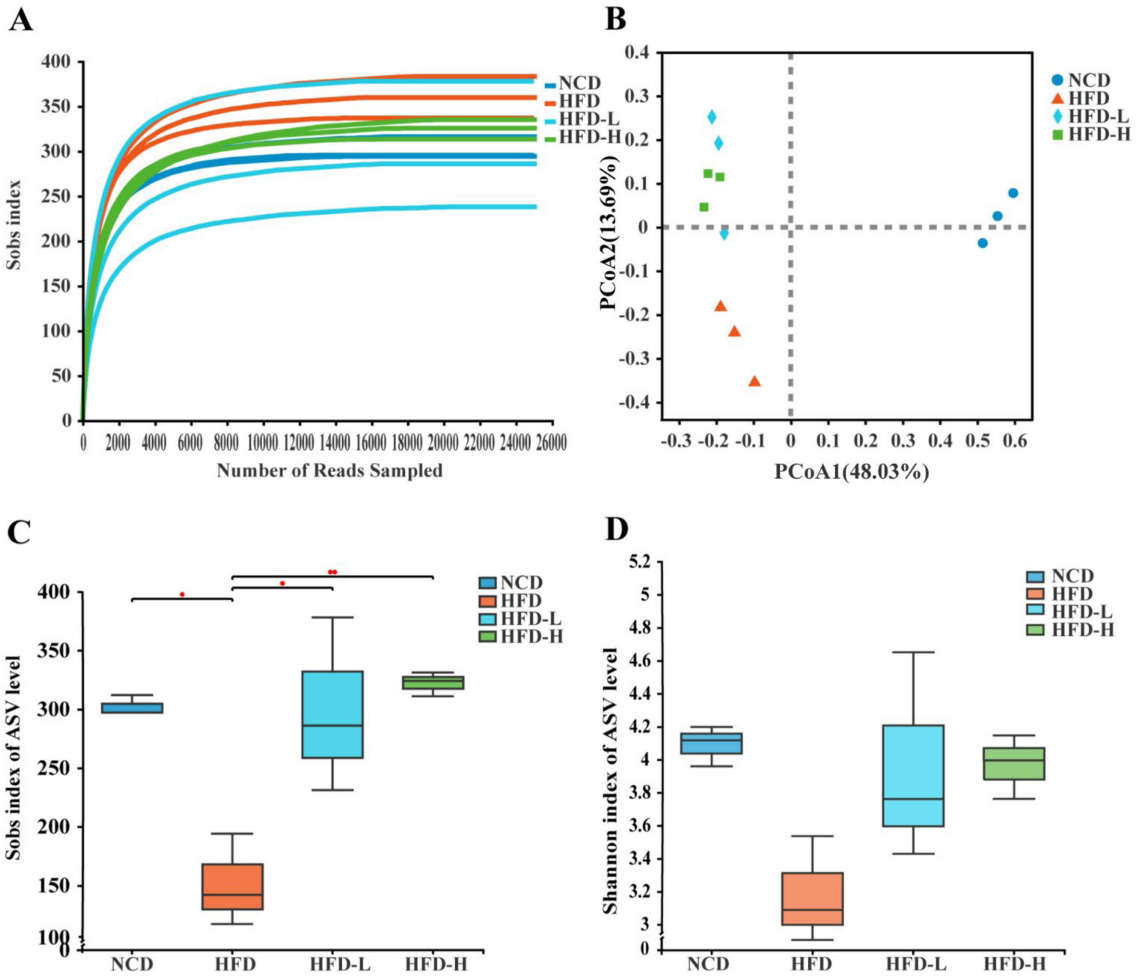

Fig. 5. *L. acidophilus* CICC 6075 altered gut microbiota richness and diversity in HFD-fed mice. (**A**) Rarefaction curve. (**B**) Beta-diversity was determined using unweighted UniFrac distance-based PCoA. (**C, D**) Effects of *L. acidophilus* CICC 6075 treatment on alpha-diversity were determined using the Sobs and Shannon indices. Data are expressed as mean ± SEM (n=3). *p<0.05 and **p<0.01. NCD: normal chow diet; HFD: high-fat diet; HFD-L: HFD-fed with *L. acidophilus*-treated group; HFD-H: HFD-fed with heat-killed *L. acidophilus*-treated group; SEM: standard error of mean.

doi: 10.12938/bmfh.2024-008

the Firmicutes/Bacteroidetes ratio and substantially increased the abundance of Actinobacteria (Fig. 6A and 6B).

Within the top 15 families, the administration of *L. acidophilus* CICC 6075 significantly enhanced the abundances of *Erysipelotrichaceae* and *Atopobiaceae* ($p<0.05$), whereas the abundance of *Peptostreptococcaceae* dropped ($p<0.05$) compared with HFD mice (Fig. 6C and 6D). At the genus level, treatment with *L. acidophilus* CICC 6075 resulted in a significant increase in *Ileibacterium* and a significant decrease in unclassified_f_*Lachnospiraceae*, unclassified_f_*Prevotellaceae*,

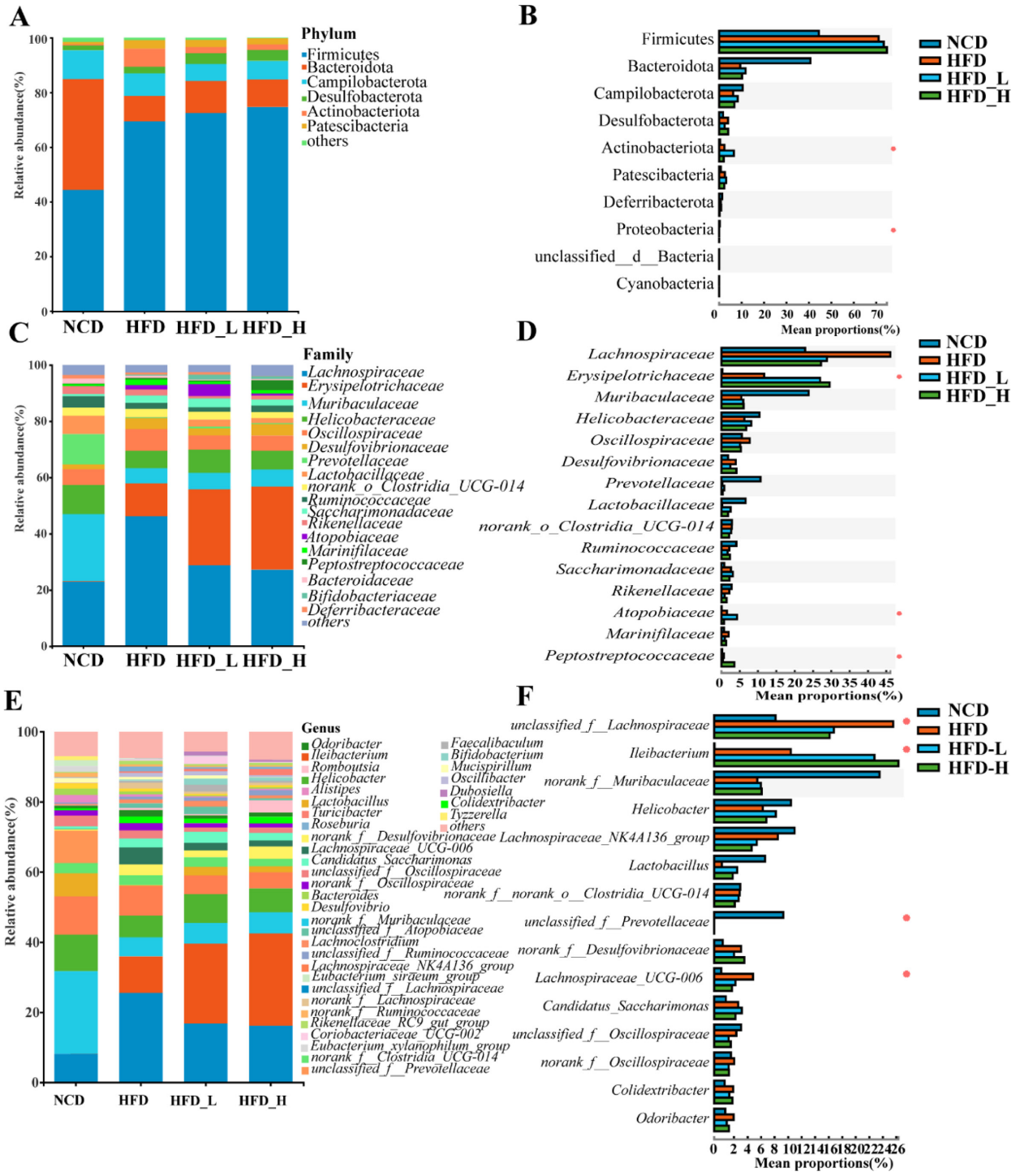

Fig. 6. *L. acidophilus* CICC 6075 altered the gut microbiota composition in HFD-fed mice. (**A**) The relative abundances of gut microbiota at the phylum level in the groups. (**B**) The relative abundances of the top 10 genera at the phylum level. (**C**) The relative abundances of gut microbiota at the family level in the groups. (**D**) The relative abundances of the top 15 genera at the family level. (**E**) The relative abundances of gut microbiota at the genus level in the groups. (**F**) The relative abundances of the top 15 genera at the genus level. Data are expressed as means ± SEM (n=3). *p<0.05; **p<0.01, and ***p<0.001 for HFD vs. HFD-L. NCD: normal chow diet; HFD: high-fat diet; HFD-L: HFD-fed with *L. acidophilus*-treated group; HFD-H: HFD-fed with heat-killed *L. acidophilus*-treated group; SEM: standard error of mean.

doi: 10.12938/bmfh.2024-008

and *Lachnospiraceae*_UCG-006 ($p<0.05$) compared with HFD mice (Fig. 6E and 6F).

Furthermore, the bacterial community structure, which exhibited significant variations across the NCD, HFD, HFD-L, and HFD-H groups, was subjected to additional analysis using the LEfSe technique (Supplementary Fig. 4A and 4B). It was found that the abundances of taxa at different levels varied among the four groups. Furthermore, unclassified_f_*Prevotellaceae*, *Muribaculum*, *Eubacterium_siraeum*_group, Gammaproteobacteria, and Proteobacteria had significant functions and might serve as biomarkers in the NCD group. Nevertheless, the unclassified_f_*Lachnospiraceae* and *Lachnospiraceae*_UCG-006 exhibited significant functionality and might serve as biomarkers in the HFD group. Actinobacteriota, Coriobacteriales, *Atopobiaceae*, *Faecalibaculum*, *Bifidobacteriaceae*, *Lachnoclostridium*, Coriobacteriia, and *Dubosiella* played important roles and could be used as biomarkers in the HFD-L group, while Erysipelotrichales, *Ileibacterium*, *Bacilli*, *Romboutsia*, *Peptostreptococcaceae*, *Turicibacter*, *Blautia*, and *Clostridiaceae* were significant biomarkers in the HFD-H group. In addition, the HFD group had a smaller number of taxa with differential abundances compared with the HFD-L and HFD-H groups. This suggests that *L. acidophilus* CICC 6075 has a restorative impact on the beneficial microbiota increase seen in the HFD group.

Effects of L. acidophilus *CICC 6075 on the gut microbiota function*

The gut microbiota plays a critical role in the physiology of the host and has a significant impact on systemic metabolism and the pathology of obesity. To explore the functional potential of bacteria in the HFD group, we used PICRUSt and analyzed data from the KEGG database to identify functional categories associated with KEGG functional categories. Based on these results, the enzymes, KO indicating functionally corresponding sets of genes, KEGG Module indicating specific biological processes and functionally related sets of genes, and hierarchical categorization of KEGG pathways (Pathways 1–3) from broad biological processes (Pathway 1) to specific biochemical pathways (Pathway 3). Compared with the NCD group, HFD feeding had a dramatic impact on the four functional categories. However, treatment with *L. acidophilus* CICC 6075 completely reversed these effects (Fig. 7A–7F). Overall, this study suggests that *L. acidophilus* CICC 6075 treatment enhances the gut microbiota functions related to metabolism, immune responses, and pathogenesis.

Histidine production by L. acidophilus *CICC 6075 reduced systemic inflammation via the NF-κB pathway and protected against obesity*

Given the significant differences in histidine biosynthesis function among the groups, serum histidine levels were assessed. As anticipated, histidine levels were significantly lower in the HFD group than in the NCD group. Histidine levels exhibited an increase in the HFD-L group, but no significant difference was observed in the HFD-H group (Fig. 8A). To further investigate the mitigating effects of histidine on obesity, serum levels of the inflammatory cytokines TNF-α, IL-6, and IL-8 were assessed. The results showed that supplementation with *L. acidophilus* CICC 6075 significantly reduced the elevated levels of TNF-α, IL-6, and IL-8 in the HFD group, whereas no significant changes were observed in the HFD-H group (Fig. 8B–8D). RT-qPCR results showed that the expression of NF-κB in adipose tissue of the HFD group was significantly higher than that of the NCD group, whereas compared with the HFD group, the expression level in the HFD-L group was significantly lower. Likewise, there were no significant differences observed between the HFD-H group and HFD group (Fig. 8E). In summary, these results suggested that supplementation of *L. acidophilus* CICC 6075 mitigated the inflammatory response in mice with HFD-induced obesity.

DISCUSSION

In this study, we performed metagenomic shotgun sequencing analysis on a cohort of healthy and obese individuals to thoroughly investigate differences in the gut microbiota. Our results show that there is a significant difference in the abundance of *L. acidophilus* between individuals with normal body mass index and those with obesity. Specifically, we observed significant differences in *L. acidophilus* abundance in obese individuals compared with healthy-weight individuals. We then demonstrated that supplementation with *L. acidophilus* CICC 6075 was effective in reducing HFD-induced obesity in mice. Kang *et al.* [24] also found similar results by evaluating the effect of *L. acidophilus* isolated from porcine intestines on obesity. However, in the present study, *L. acidophilus* was obtained by analyzing the metagenomic results from patients with obesity, and this provided the first insight into the effect of *L. acidophilus* CICC 6075 HFD-induced obesity.

Metagenomic data showed that obese individuals have significant differences in the gut microbiome and decreased alpha-diversity compared with healthy individuals. This is consistent with the findings of Kim *et al.* [43], who found that gut microbial diversity in patients with obesity with metabolic disorders decreased. Depletion of beneficial bacteria is accompanied by the progression of obesity. We compared abundance of *Lactobacillus* spp. at the species level between healthy individuals and patients with obesity and found *L. acidophilus* decreased significantly in patients with obesity. In addition, *L. acidophilus* CICC 6075 can reduce inflammation levels and oxidative stress in atherosclerotic mice [44, 45]. The study also found that supplementation with *L. acidophilus* CICC 6075 improved the intestinal microbial structure, significantly reduced the abundance of pathogenic *Helicobacter*, and increased the abundance of beneficial *Lachnospiraceae*_NK4A136_group [46]. This reveals that *L. acidophilus* CICC 6075 has potential anti-obesity effects. Our results show that supplementation with live *L. acidophilus* CICC 6075 could effectively alleviate obesity, which has not been reported in previous obesity studies. In HFD-induced animal models, changes in intestinal microecology lead to intestinal barrier destruction, and LPS produced by gram-negative bacteria are more likely to enter the liver and intestinal circulation through the leaky gut tract and cause inflammation. After supplementation with *L. acidophilus* CICC 6075, the expression of intestinal tight junction proteins in obese mice increased, and the expression levels of IL-6 and IL-8 were significantly reduced. These results showed that supplementation with *L. acidophilus* CICC 6075 effectively maintained the damaged intestinal barrier.

Previous studies have shown that probiotic supplementation is associated with changes in intestinal microbiota, and the results of this study support this conclusion. Probiotics can promote the

proliferation of beneficial bacteria and inhibit the reproduction of harmful bacteria, balancing the intestinal microbiota. Therefore, we investigated significant changes in the intestinal microbiota. Although previous studies have shown that *L. acidophilus* CICC 6075 significantly alleviates HFD-induced chronic inflammatory diseases, intestinal microbes were not detected herein, and we remedied this deficiency. The ratio of Firmicutes to Bacteroides increases in the guts of obese individuals and HFD-induced animal models, and these critical phyla play a role in obesity-related inflammation [47, 48]. The results herein showed that supplementation with *L. acidophilus* CICC 6075 significantly reversed intestinal flora disorders and restored the ratio of Firmicutes to Bacteroidetes.

Additionally, HFD-induced obesity reduces *Ileibacterium* spp., and the abundance of these bacteria is negatively correlated with chronic inflammatory diseases, such as obesity and atherosclerosis,

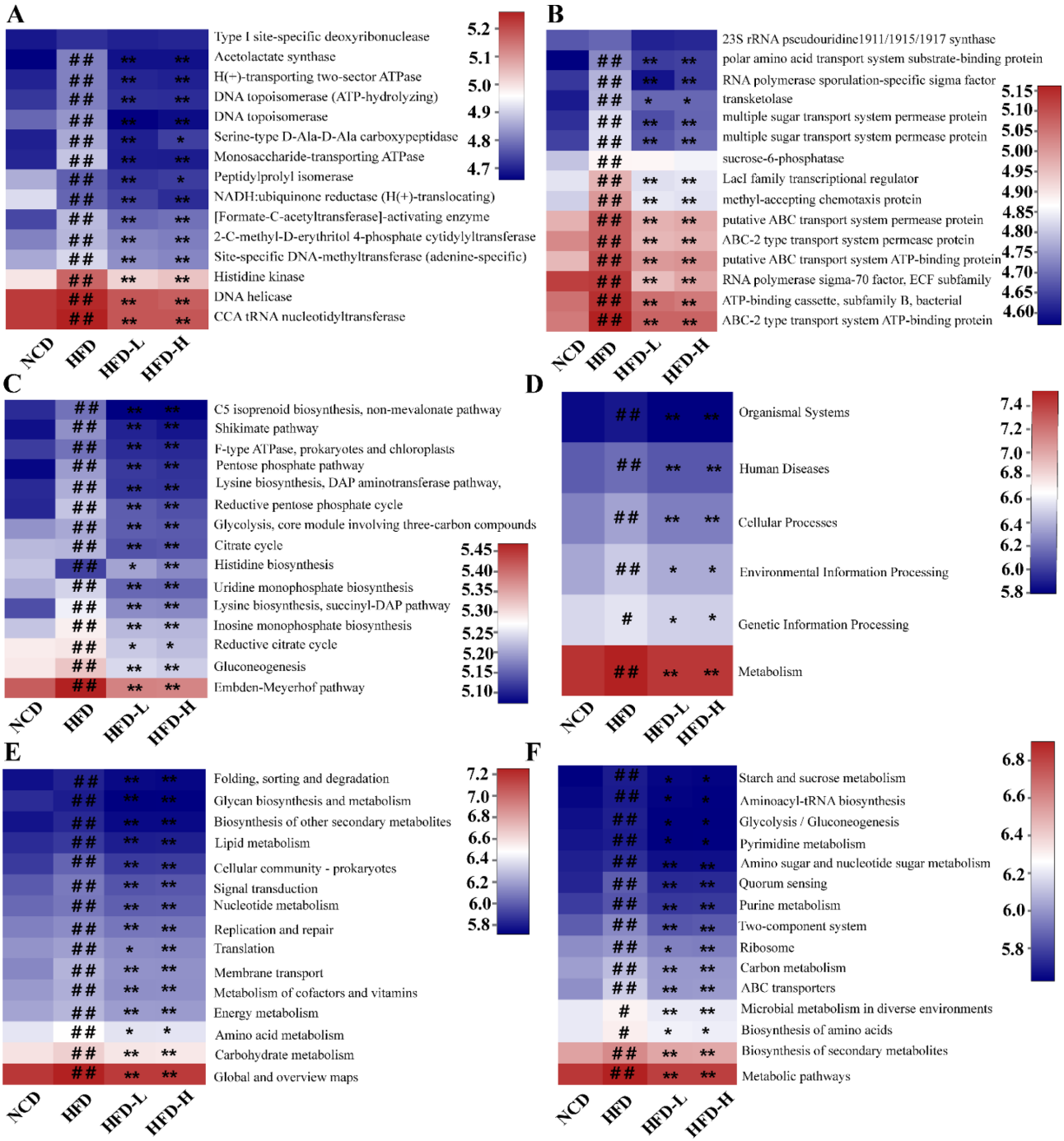

Fig. 7. Effect of *L. acidophilus* CICC 6075 on gut microbiota function in HFD-fed mice based on the KEGG database. Effects of *L. acidophilus* CICC 6075 treatment on (**A**) enzymes, (**B**) KOs, (**C**) modules, (**D**) pathway 1, (**E**) pathway 2, and (**F**) pathway 3. $^{\#}p<0.05$, $^{\#\#}p<0.01$, and $^{\#\#\#}p<0.001$ vs. NCD; $^{*}p<0.05$; $^{**}p<0.01$, and $^{***}p<0.001$ vs. HFD-L and HFD-H. NCD: normal chow diet; HFD: high-fat diet; HFD-L: HFD-fed with *L. acidophilus*-treated group; HFD-H: HFD-fed with heat-killed *L. acidophilus*-treated group; SEM: standard error of mean.

doi: 10.12938/bmfh.2024-008

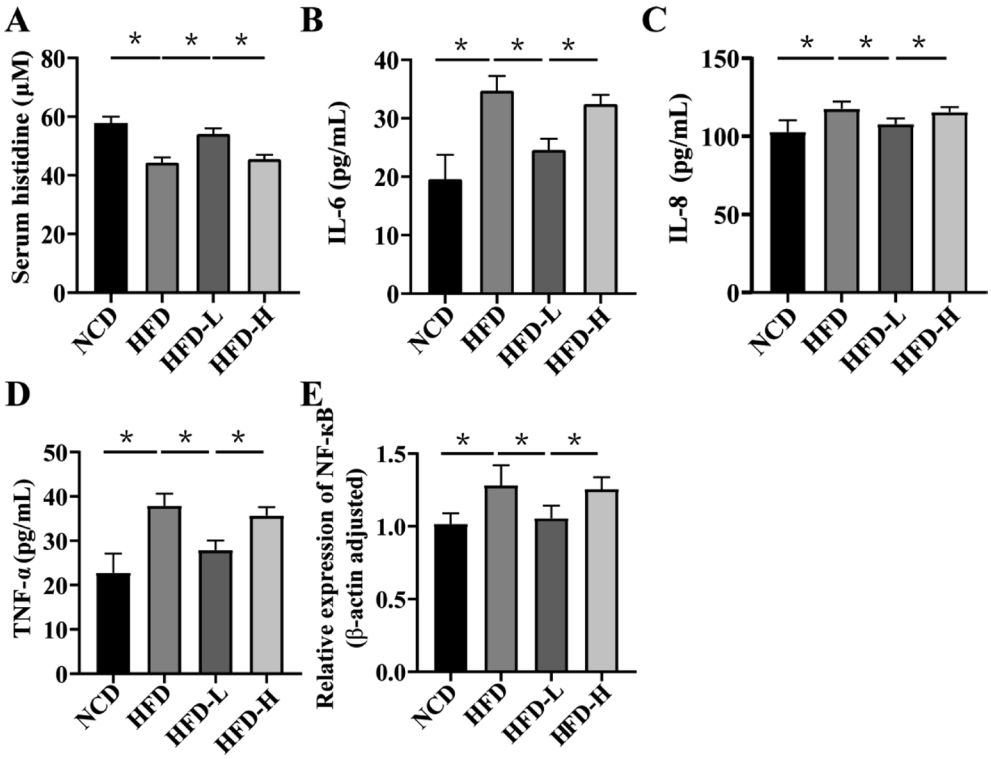

Fig. 8. *L. acidophilus* CICC 6075 produced histidine to reduce systemic inflammation via the NF-κB pathway and prevented obesity. **(A)** Serum histidine concentrations in different groups. Statistical analysis of (**B**) IL-6, (**C**) IL-8, and (**D**) TNF-α levels in serum of the four groups of mice. (**E**) Statistical analysis of NF-κB mRNA expression of mouse adipose tissue in the four groups. Data are expressed as mean ± SEM (n=3). *p<0.05; **p<0.01, and ***p<0.001. NCD: normal chow diet; HFD: high-fat diet; HFD-L: HFD-fed with *L. acidophilus*-treated group; HFD-H: HFD-fed with heat-killed *L. acidophilus*-treated group; SEM: standard error of mean.

and aging [49–51]. It has been reported that *Helicobacter* is negatively correlated with intestinal tight junction protein expression, which increases after HFD feeding [52]. Furthermore, we described the association between HFD-induced obesity and *Helicobacter*, whose abundance did not increase significantly after HFD feeding [53, 54]. *Lachnospiraceae*_UCG-006 is associated with HFD-induced obesity [55], which is consistent with our results. Supplementation with *L. acidophilus* CICC 6075 reduces the abundance of *Lachnospiraceae*_UCG-006 [55]. These results suggest that increasing the abundance of some beneficial bacteria and reducing bacteria associated with inflammation or obesity is partly responsible for the relief of obesity with *L. acidophilus* supplementation. Thus, supplementation with *L. acidophilus* CICC 6075 can alleviate HFD-induced obesity and improve the composition of the gut microbiota.

Moreover, predictions of the bacterial functional potential of the gut microbiome varied significantly across groups, and *L. acidophilus* CICC 6075 supplementation reduced HFD-mediated inflammatory responses, energy metabolism, immune responses, and pathogenic gut microbiota dysfunction to levels observed in mice fed a normal diet. Furthermore, it was revealed that a possible reason for supplementation with *L. acidophilus* CICC 6075 maintaining gut homeostasis is the induction of functional changes via an altered gut microbial composition, thereby enabling new interactions between microbes, metabolites, and the immunity of the host.

It has been reported in animal studies that probiotics such as *Lachnospiraceae*_NK4A136_group and unclassified_f_*Lachnospiraceae* are involved in the production short-chain fatty acids, maintenance of gut barrier integrity, and inhibition of inflammatory responses, indicating their potential in combating obesity [56–60]. Our results revealed that compared with the HFD-L group, the abundances of *Lachnospiraceae*_NK4A136_group and unclassified_f_*Lachnospiraceae* were reduced in the HFD-H group. This suggests that supplementation of heat-killed probiotics impedes the ability of the microbiota to restore its functionality, thereby reversing the anti-obesity effects of probiotics.

Furthermore, histidine, a key molecular regulator of lipid metabolism, is known to be reduced in individuals with obesity and type 2 diabetes [61–63]. It plays a role in inhibiting inflammation and oxidative stress via the NF-κB pathway, thereby improving insulin resistance [29, 64–66]. An untargeted metabolomics study of *L. acidophilus* showed that *L.acidophilus* was significantly associated with amino acid metabolism, including histidine metabolism, arginine metabolism, and threonine metabolism, which is consistent with our findings [67]. In this study, supplementation of *L. acidophilus* CICC 6075 enhanced histidine biosynthesis and suppressed the NF-κB inflammatory signaling pathway. However, supplementation of heat-killed *L. acidophilus* CICC 6075 failed to exert the same effects. This suggests that the inability of heat-killed *L. acidophilus* CICC 6075 to effectively alleviate obesity may be attributed to impaired regulation of metabolism, resulting in NF-κB activation and systemic inflammation that counteracts the anti-obesity effects of probiotics.

In conclusion, *L. acidophilus* CICC 6075 alleviates HFD-induced obesity in mice by inhibiting the activation of the NF-κB pathway and enhancing gut microbiota functionality. This study provides novel insights for the future treatment of obesity.

PREPRINT PUBLICATION

The preprint entitled "*Lactobacillus acidophilus* CICC 6075 Attenuates HFD-induced Obesity by Improving Gut Microbiota Composition and Histidine Biosynthesis" was posted in the Research Square repository on 30 January 2024, DOI: https://doi.org/10.21203/rs.3.rs-2195035/v2.

ETHICS APPROVAL

This study protocol was reviewed and approved by the Ethical Guidelines of Xuzhou Medical University Laboratory Animal Ethics Management Committee (approval number 4120185).

AVAILABILITY OF DATA AND MATERIALS

The datasets generated during the current study are available in the figshare repository, https://figshare.com/s/9d51adc1a6ede8398a36.

AUTHOR CONTRIBUTIONS

Conceptualization, ZW and RC. Methodology, ZW. Software, SY. Validation, SZ, YZ, DY and XG. Data curation, SY, YW. Writing—original draft preparation, YZ and SY. Visualization, SY. Project administration, ZW. Funding acquisition, RC. All authors contributed to the article and approved the submitted version.

FUNDING

Key University Science Research Project of Jiangsu Province (22KJA320005); The Jiangsu Planned Projects for Postdoctoral Research Foundation (1501010B); the China Postdoctoral Science Foundation (2016M590506); Jiangsu Province College Students' Innovation And Entrepreneurship Training Program (202110313073Y); Jiangsu Key Laboratory of Animal genetic Breeding and Molecular Design (AGBMD2020001); Medical Guidance Program of Jiangsu Provincial Health and Wellness Commission (Z2023091); and Xuzhou Key R&D Program (Social Development)-Medicine and Health Surface Project (KC23277).

CONFLICT OF INTEREST

The authors declare no competing interests.

REFERENCES

1. Kolotkin RL, Meter K, Williams GR. 2001. Quality of life and obesity. Obes Rev 2: 219–229. [Medline] [CrossRef]
2. Caballero B. 2019. Humans against obesity: who will win? Adv Nutr 10 suppl_1: S4–S9. [Medline] [CrossRef]
3. Conway B, Rene A. 2004. Obesity as a disease: no lightweight matter. Obes Rev 5: 145–151. [Medline] [CrossRef]
4. Saltiel AR, Olefsky JM. 2017. Inflammatory mechanisms linking obesity and metabolic disease. J Clin Invest 127: 1–4. [Medline] [CrossRef]
5. Bendor CD, Bardugo A, Pinhas-Hamiel O, Afek A, Twig G. 2020. Cardiovascular morbidity, diabetes and cancer risk among children and adolescents with severe obesity. Cardiovasc Diabetol 19: 79. [Medline] [CrossRef]
6. Srivastava G, Apovian C. 2018. Future pharmacotherapy for obesity: new anti-obesity drugs on the horizon. Curr Obes Rep 7: 147–161. [Medline] [CrossRef]
7. Saunders KH, Umashanker D, Igel LI, Kumar RB, Aronne LJ. 2018. Obesity pharmacotherapy. Med Clin North Am 102: 135–148. [Medline] [CrossRef]
8. Son JW, Kim S. 2020. Comprehensive review of current and upcoming anti-obesity drugs. Diabetes Metab J 44: 802–818. [Medline] [CrossRef]
9. Molina-Tijeras JA, Diez-Echave P, Vezza T, Hidalgo-García L, Ruiz-Malagón AJ, Rodríguez-Sojo MJ, Romero M, Robles-Vera I, García F, Plaza-Diaz J, *et al.* 2021. *Lactobacillus fermentum* CECT5716 ameliorates high fat diet-induced obesity in mice through modulation of gut microbiota dysbiosis. Pharmacol Res 167: 105471. [Medline] [CrossRef]
10. Hauner H. 2021. [Obesity treatment-legal and illegal drugs and the future]. Internist (Berl) 62: 1354–1359 (in German). [Medline] [CrossRef]
11. Rosenbaum M, Knight R, Leibel RL. 2015. The gut microbiota in human energy homeostasis and obesity. Trends Endocrinol Metab 26: 493–501. [Medline] [CrossRef]
12. Liu X, Zhao K, Jing N, Kong Q, Yang X. 2021. Epigallocatechin Gallate (EGCG) promotes the immune function of ileum in high fat diet fed mice by regulating gut microbiome profiling and immunoglobulin production. Front Nutr 8: 720439. [Medline] [CrossRef]
13. Sonnenburg JL, Bäckhed F. 2016. Diet-microbiota interactions as moderators of human metabolism. Nature 535: 56–64. [Medline] [CrossRef]
14. Gomes AC, Hoffmann C, Mota JF. 2018. The human gut microbiota: metabolism and perspective in obesity. Gut Microbes 9: 308–325. [Medline]
15. Tseng CH, Wu CY. 2019. The gut microbiome in obesity. J Formos Med Assoc 118 Suppl 1: S3–S9. [Medline] [CrossRef]
16. Miyamoto J, Igarashi M, Watanabe K, Karaki SI, Mukouyama H, Kishino S, Li X, Ichimura A, Irie J, Sugimoto Y, *et al.* 2019. Gut microbiota confers host resistance to obesity by metabolizing dietary polyunsaturated fatty acids. Nat Commun 10: 4007. [Medline] [CrossRef]
17. Canfora EE, Meex RCR, Venema K, Blaak EE. 2019. Gut microbial metabolites in obesity, NAFLD and T2DM. Nat Rev Endocrinol 15: 261–273. [Medline] [CrossRef]
18. Ondee T, Pongpirul K, Visitchanakun P, Saisorn W, Kanacharoen S, Wongsaroj L, Kullapanich C, Ngamwongsatit N, Settachaimongkon S, Somboonna N, *et al.* 2021. *Lactobacillus acidophilus* LA5 improves saturated fat-induced obesity mouse model through the enhanced intestinal *Akkermansia muciniphila*. Sci Rep 11: 6367. [Medline] [CrossRef]
19. Amdekar S, Singh V, Kumar A, Sharma P, Singh R. 2014. *Lactobacillus acidophilus* protected organs in experimental arthritis by regulating the pro-inflammatory cytokines. Indian J Clin Biochem 29: 471–478. [Medline] [CrossRef]
20. Cavalcanti Neto MP, Aquino JS, Romão da Silva LF, de Oliveira Silva R, Guimarães KSL, de Oliveira Y, de Souza EL, Magnani M, Vidal H, de Brito Alves JL. 2018. Gut microbiota and probiotics intervention: a potential therapeutic target for management of cardiometabolic disorders and chronic kidney disease? Pharmacol Res 130: 152–163. [Medline] [CrossRef]
21. Park SS, Lee YJ, Song S, Kim B, Kang H, Oh S, Kim E. 2018. *Lactobacillus acidophilus* NS1 attenuates diet-induced obesity and fatty liver. J Endocrinol 237: 87–100. [Medline] [CrossRef]
22. Song M, Park S, Lee H, Min B, Jung S, Park S, Kim E, Oh S. 2015. Effect of *Lactobacillus acidophilus* NS1 on plasma cholesterol levels in diet-induced obese mice. J Dairy Sci 98: 1492–1501. [Medline] [CrossRef]
23. Park SS, Yang G, Kim E. 2017. *Lactobacillus acidophilus* NS1 reduces phosphoenolpyruvate carboxylase expression by regulating HNF4α transcriptional activity. Han-gug Chugsan Sigpum Hag-hoeji 37: 529–534. [Medline]
24. Kang Y, Kang X, Yang H, Liu H, Yang X, Liu Q, Tian H, Xue Y, Ren P, Kuang X, *et al.* 2022. *Lactobacillus acidophilus* ameliorates obesity in mice through modulation of gut microbiota dysbiosis and intestinal permeability. Pharmacol Res 175: 106020. [Medline] [CrossRef]
25. Zhang X, Yao C, Wang T, Zhao H, Zhang B. 2021. Production of high-purity galacto-oligosaccharides (GOS) by *Lactobacillus*-derived β-galactosidase. Eur Food Res Technol 247: 1501–1510. [CrossRef]
26. Lee G, Kim YY, Jang H, Han JS, Nahmgoong H, Park YJ, Han SM, Cho C, Lim S, Noh JR, *et al.* 2022. SREBP1c-PARP1 axis tunes anti-senescence activity of adipocytes and ameliorates metabolic imbalance in obesity. Cell Metab 34: 702–718.e5. [Medline] [CrossRef]
27. Vera-Aviles M, Vantana E, Kardinasari E, Koh NL, Latunde-Dada GO. 2018. Protective role of histidine supplementation against oxidative stress damage in the management of anemia of chronic kidney disease. Pharmaceuticals (Basel) 11: 111. [Medline] [CrossRef]
28. Hayashi T, Yamashita T, Takahashi T, Tabata T, Watanabe H, Gotoh Y, Shinohara M, Kami K, Tanaka H, Matsumoto K, *et al.* 2021. Uncovering the role of gut microbiota in amino acid metabolic disturbances in heart failure through metagenomic analysis. Front Cardiovasc Med 8: 789325. [Medline] [CrossRef]
29. Menon K, Marquina C, Liew D, Mousa A, de Courten B. 2020. Histidine-containing dipeptides reduce central obesity and improve glycaemic outcomes: a systematic review and meta-analysis of randomized controlled trials. Obes Rev 21: e12975. [Medline] [CrossRef]

30. Yan SL, Wu ST, Yin MC, Chen HT, Chen HC. 2009. Protective effects from carnosine and histidine on acetaminophen-induced liver injury. J Food Sci 74: H259–H265. [Medline] [CrossRef]
31. Mayneris-Perxachs J, Cardellini M, Hoyles L, Latorre J, Davato F, Moreno-Navarrete JM, Arnoriaga-Rodríguez M, Serino M, Abbott J, Barton RH, *et al.* 2021. Iron status influences non-alcoholic fatty liver disease in obesity through the gut microbiome. Microbiome 9: 104. [Medline] [CrossRef]
32. DiNicolantonio JJ, McCarty MF, OKeefe JH. 2018. Role of dietary histidine in the prevention of obesity and metabolic syndrome. Open Heart 5: e000676. [Medline] [CrossRef]
33. Liu R, Hong J, Xu X, Feng Q, Zhang D, Gu Y, Shi J, Zhao S, Liu W, Wang X, *et al.* 2017. Gut microbiome and serum metabolome alterations in obesity and after weight-loss intervention. Nat Med 23: 859–868. [Medline] [CrossRef]
34. Hoyles L, Fernández-Real JM, Federici M, Serino M, Abbott J, Charpentier J, Heymes C, Luque JL, Anthony E, Barton RH, *et al.* 2018. Molecular phenomics and metagenomics of hepatic steatosis in non-diabetic obese women. Nat Med 24: 1070–1080. [Medline] [CrossRef]
35. Kleiner DE, Makhlouf HR. 2016. Histology of nonalcoholic fatty liver disease and nonalcoholic steatohepatitis in adults and children. Clin Liver Dis 20: 293–312. [Medline] [CrossRef]
36. Hall M, Beiko RG. 2018. 16S rRNA gene analysis with QIIME2. Methods Mol Biol 1849: 113–129. [Medline] [CrossRef]
37. Langille MGI, Zaneveld J, Caporaso JG, McDonald D, Knights D, Reyes JA, Clemente JC, Burkepile DE, Vega Thurber RL, Knight R, *et al.* 2013. Predictive functional profiling of microbial communities using 16S rRNA marker gene sequences. Nat Biotechnol 31: 814–821. [Medline] [CrossRef]
38. Cani PD, Bibiloni R, Knauf C, Waget A, Neyrinck AM, Delzenne NM, Burcelin R. 2008. Changes in gut microbiota control metabolic endotoxemia-induced inflammation in high-fat diet-induced obesity and diabetes in mice. Diabetes 57: 1470–1481. [Medline] [CrossRef]
39. Ley RE, Turnbaugh PJ, Klein S, Gordon JI. 2006. Microbial ecology: human gut microbes associated with obesity. Nature 444: 1022–1023. [Medline] [CrossRef]
40. Brun P, Castagliuolo I, Di Leo V, Buda A, Pinzani M, Palù G, Martines D. 2007. Increased intestinal permeability in obese mice: new evidence in the pathogenesis of nonalcoholic steatohepatitis. Am J Physiol Gastrointest Liver Physiol 292: G518–G525. [Medline] [CrossRef]
41. Kang Y, Li Y, Du Y, Guo L, Chen M, Huang X, Yang F, Hong J, Kong X. 2019. Konjaku flour reduces obesity in mice by modulating the composition of the gut microbiota. Int J Obes (Lond) 43: 1631–1643. [Medline] [CrossRef]
42. Everard A, Lazarevic V, Derrien M, Girard M, Muccioli GG, Neyrinck AM, Possemiers S, Van Holle A, François P, de Vos WM, *et al.* 2011. Responses of gut microbiota and glucose and lipid metabolism to prebiotics in genetic obese and diet-induced leptin-resistant mice. Diabetes 60: 2775–2786. [Medline] [CrossRef]
43. Kim MH, Yun KE, Kim J, Park E, Chang Y, Ryu S, Kim HL, Kim HN. 2020. Gut microbiota and metabolic health among overweight and obese individuals. Sci Rep 10: 19417. [Medline] [CrossRef]
44. Lin MY, Chang FJ. 2000. Antioxidative effect of intestinal bacteria *Bifidobacterium longum* ATCC 15708 and Lactobacillus acidophilus ATCC 4356. Dig Dis Sci 45: 1617–1622. [Medline] [CrossRef]
45. Chen L, Liu W, Li Y, Luo S, Liu Q, Zhong Y, Jian Z, Bao M. 2013. *Lactobacillus acidophilus* ATCC 4356 attenuates the atherosclerotic progression through modulation of oxidative stress and inflammatory process. Int Immunopharmacol 17: 108–115. [Medline] [CrossRef]
46. Zhang P, Han X, Zhang X, Zhu X. 2021. *Lactobacillus acidophilus* ATCC 4356 alleviates renal ischemia-reperfusion injury through antioxidant stress and anti-inflammatory responses and improves intestinal microbial distribution. Front Nutr 8: 667695. [Medline] [CrossRef]
47. Turnbaugh PJ, Hamady M, Yatsunenko T, Cantarel BL, Duncan A, Ley RE, Sogin ML, Jones WJ, Roe BA, Affourtit JP, *et al.* 2009. A core gut microbiome in obese and lean twins. Nature 457: 480–484. [Medline] [CrossRef]
48. Neyrinck AM, Possemiers S, Druart C, Van de Wiele T, De Backer F, Cani PD, Larondelle Y, Delzenne NM. 2011. Prebiotic effects of wheat arabinoxylan related to the increase in bifidobacteria, *Roseburia* and *Bacteroides/Prevotella* in diet-induced obese mice. PLoS One 6: e20944. [Medline] [CrossRef]
49. Lan Y, Ma Z, Chang L, Peng J, Zhang M, Sun Q, Qiao R, Hou X, Ding X, Zhang Q, *et al.* 2023. Sea buckthorn polysaccharide ameliorates high-fat diet induced mice neuroinflammation and synaptic dysfunction via regulating gut dysbiosis. Int J Biol Macromol 236: 123797. [Medline] [CrossRef]
50. Xie B, Zu X, Wang Z, Xu X, Liu G, Liu R. 2022. Ginsenoside Rc ameliorated atherosclerosis *via* regulating gut microbiota and fecal metabolites. Front Pharmacol 13: 990476. [Medline] [CrossRef]
51. Meng Y, Meng Q, Li C, Wang M, Li S, Ying J, Zheng H, Bai S, Xue Y, Shen Q. 2023. A comparison between partially peeled hulless barley and whole grain hulless barley: beneficial effects on the regulation of serum glucose and the gut microbiota in high-fat diet-induced obese mice. Food Funct 14: 886–898. [Medline] [CrossRef]
52. Choi S, Kim N, Park JH, Nam RH, Song CH, Lee HS. 2022. Effect of Helicobacter pylori infection and its eradication on the expression of tight junction proteins in the gastric epithelium in relation to gastric carcinogenesis. Helicobacter 27: e12929. [Medline] [CrossRef]
53. Okushin K, Takahashi Y, Yamamichi N, Shimamoto T, Enooku K, Fujinaga H, Tsutsumi T, Shintani Y, Sakaguchi Y, Ono S, *et al.* 2015. *Helicobacter pylori* infection is not associated with fatty liver disease including non-alcoholic fatty liver disease: a large-scale cross-sectional study in Japan. BMC Gastroenterol 15: 25. [Medline] [CrossRef]
54. Baeg MK, Yoon SK, Ko SH, Noh YS, Lee IS, Choi MG. 2016. *Helicobacter pylori* infection is not associated with nonalcoholic fatty liver disease. World J Gastroenterol 22: 2592–2600. [Medline] [CrossRef]
55. Li X, Wang Y, Xing Y, Xing R, Liu Y, Xu Y. 2020. Changes of gut microbiota during silybin-mediated treatment of high-fat diet-induced non-alcoholic fatty liver disease in mice. Hepatol Res 50: 5–14. [Medline] [CrossRef]
56. Ma L, Ni Y, Wang Z, Tu W, Ni L, Zhuge F, Zheng A, Hu L, Zhao Y, Zheng L, *et al.* 2020. Spermidine improves gut barrier integrity and gut microbiota function in diet-induced obese mice. Gut Microbes 12: 1–19. [Medline] [CrossRef]
57. Wang P, Li D, Ke W, Liang D, Hu X, Chen F. 2020. Resveratrol-induced gut microbiota reduces obesity in high-fat diet-fed mice. Int J Obes (Lond) 44: 213–225. [Medline] [CrossRef]
58. Wang P, Gao J, Ke W, Wang J, Li D, Liu R, Jia Y, Wang X, Chen X, Chen F, *et al.* 2020. Resveratrol reduces obesity in high-fat diet-fed mice via modulating the composition and metabolic function of the gut microbiota. Free Radic Biol Med 156: 83–98. [Medline] [CrossRef]
59. Yu G, Ji X, Huang J, Liao A, Pan L, Hou Y, Hui M, Guo W. 2021. Immunity improvement and gut microbiota remodeling of mice by wheat germ globulin. World J Microbiol Biotechnol 37: 64. [Medline] [CrossRef]
60. Li M, Zhao Y, Wang Y, Geng R, Fang J, Kang SG, Huang K, Tong T. 2022. Eugenol, a major component of clove oil, attenuates adiposity, and modulates gut microbiota in high-fat diet-fed mice. Mol Nutr Food Res 66: e2200387. [Medline] [CrossRef]
61. Niu YC, Feng RN, Hou Y, Li K, Kang Z, Wang J, Sun CH, Li Y. 2012. Histidine and arginine are associated with inflammation and oxidative stress in obese women. Br J Nutr 108: 57–61. [Medline] [CrossRef]
62. Hu X, Guo F. 2021. Amino acid sensing in metabolic homeostasis and health. Endocr Rev 42: 56–76. [Medline] [CrossRef]
63. Aron-Wisnewsky J, Warmbrunn MV, Nieuwdorp M, Clément K. 2021. Metabolism and metabolic disorders and the microbiome: the intestinal microbiota associated with obesity, lipid metabolism, and metabolic health-pathophysiology and therapeutic strategies. Gastroenterology 160: 573–599. [Medline] [CrossRef]
64. Feng RN, Niu YC, Sun XW, Li Q, Zhao C, Wang C, Guo FC, Sun CH, Li Y. 2013. Histidine supplementation improves insulin resistance through suppressed inflammation in obese women with the metabolic syndrome: a randomised controlled trial. Diabetologia 56: 985–994. [Medline] [CrossRef]
65. Flores V, Spicer AB, Sonsalla MM, Richardson NE, Yu D, Sheridan GE, Trautman ME, Babygirija R, Cheng EP, Rojas JM, *et al.* 2023. Regulation of metabolic health by dietary histidine in mice. J Physiol 601: 2139–2163. [Medline] [CrossRef]
66. Sun X, Feng R, Li Y, Lin S, Zhang W, Li Y, Sun C, Li S. 2014. Histidine supplementation alleviates inflammation in the adipose tissue of high-fat diet-induced obese rats via the NF-κB- and PPARγ-involved pathways. Br J Nutr 112: 477–485. [Medline] [CrossRef]
67. Guo Y, Liu X, Huang H, Lu Y, Ling X, Mo Y, Yin C, Zhu H, Zheng H, Liang Y, *et al.* 2022. Metabolic response of *Lactobacillus acidophilus* exposed to amoxicillin. J Antibiot (Tokyo) 75: 268–281. [Medline] [CrossRef]

